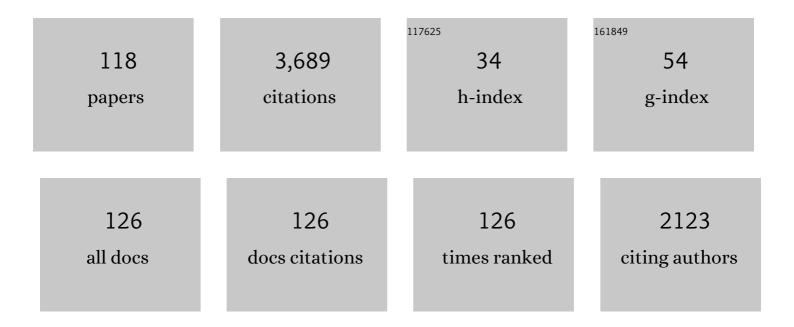
## Nicolas Clavier

List of Publications by Year in descending order

Source: https://exaly.com/author-pdf/1442036/publications.pdf Version: 2024-02-01



#	Article	IF	CITATIONS
1	Impact of impurities on the fabrication and performances of yttrium-doped thoria electrolyte ceramics. Journal of Nuclear Materials, 2022, 560, 153499.	2.7	2
2	A multiscale <i>in situ</i> high temperature high resolution transmission electron microscopy study of ThO <sub>2</sub> sintering. Nanoscale, 2021, 13, 7362-7374.	5.6	6
3	The Role of Water and Hydroxyl Groups in the Structures of Stetindite and Coffinite, MSiO <sub>4</sub> (M = Ce, U). Inorganic Chemistry, 2021, 60, 718-735.	4.0	18
4	Effect of Annealing on Structural and Thermodynamic Properties of ThSiO <sub>4</sub> -ErPO <sub>4</sub> Xenotime Solid Solution. Inorganic Chemistry, 2021, 60, 12020-12028.	4.0	2
5	SEraMic: A semi-automatic method for the segmentation of grain boundaries. Journal of the European Ceramic Society, 2021, 41, 5349-5358.	5.7	6
6	Influence of the PuO2 content on the sintering behaviour of UO2-PuO2 freeze-granulated powders under reducing conditions. Journal of the European Ceramic Society, 2021, 41, 6778-6783.	5.7	3
7	Direct sintering of UO2+x oxides prepared under hydrothermal conditions. Journal of the European Ceramic Society, 2021, 41, 6697-6707.	5.7	3
8	Reaction sintering of rhabdophane into monazite-cheralite Nd1-2xThxCaxPO4 (x = 0 – 0.1) ceramics. Journal of the European Ceramic Society, 2020, 40, 911-922.	5.7	11
9	Sintering of a UO2-PuO2 freeze-granulated powder under reducing conditions. Journal of the European Ceramic Society, 2020, 40, 5900-5908.	5.7	6
10	Hydrothermal Conversion of Thorium Oxalate into ThO <sub>2</sub> · <i>n</i> H <sub>2</sub> O Oxide. Inorganic Chemistry, 2020, 59, 14954-14966.	4.0	13
11	Early stages of UO2+x sintering by in situ high-temperature environmental scanning electron microscopy. Journal of the European Ceramic Society, 2020, 40, 5891-5899.	5.7	5
12	Charge compensation mechanisms in Nd-doped UO2 samples for stoichiometric and hypo-stoichiometric conditions: Lack of miscibility gap. Journal of Nuclear Materials, 2020, 539, 152276.	2.7	21
13	Structural changes of Nd- and Ce-doped ammonium diuranate microspheres during the conversion to U1â^'LnO2±. Journal of Nuclear Materials, 2020, 542, 152454.	2.7	2
14	Structural and Thermodynamic Investigation of the Perovskite Ba <sub>2</sub> NaMoO <sub>5.5</sub> . Inorganic Chemistry, 2020, 59, 6120-6130.	4.0	1
15	Oxidation as an Early Stage in the Multistep Thermal Decomposition of Uranium(IV) Oxalate into U3O8. Inorganic Chemistry, 2020, 59, 8589-8602.	4.0	14
16	Uranium removal from mining water using Cu substituted hydroxyapatite. Journal of Hazardous Materials, 2020, 392, 122501.	12.4	43
17	Impact of liquid sodium corrosion on microstructure and electrical properties of yttrium-doped thoria prepared by co-precipitation. Corrosion Science, 2020, 171, 108721.	6.6	4
18	Hydrothermal Conversion of Uranium(IV) Oxalate into Oxides: A Comprehensive Study. Inorganic Chemistry, 2020, 59, 3260-3273.	4.0	24

#	Article	lF	CITATIONS
19	Synthesis, Crystal Structure, and Enthalpies of Formation of Churchite-type REPO <sub>4</sub> ·2H <sub>2</sub> O (RE = Gd to Lu) Materials. Crystal Growth and Design, 2019, 19, 4641-4649.	3.0	20
20	First Stage of Sintering of ThO2 Microspheres: a HT-ESEM and HT-HRTEM Study. Microscopy and Microanalysis, 2019, 25, 49-50.	0.4	0
21	From Th-Rhabdophane to Monazite-Cheralite Solid Solutions: Thermal Behavior of Nd <sub>1–2<i>x</i></sub> Th <sub><i>x</i></sub> Ca <sub><i>x</i></sub> PO <sub>4</sub> · <i>n</i> H <sub>2 (<i>x</i> = 0–0.15). Crystal Growth and Design, 2019, 19, 2794-2801.</sub>	28 <b>/o</b> ub>0	9
22	Working with the ESEM at high temperature. Materials Characterization, 2019, 151, 15-26.	4.4	29
23	Impact of the cationic homogeneity on Th0.5U0.5O2 densification and chemical durability. Journal of Nuclear Materials, 2019, 514, 368-379.	2.7	5
24	Direct synthesis of pure brannerite UTi2O6. Journal of Nuclear Materials, 2019, 515, 401-406.	2.7	12
25	Determination of the isotopic composition of single subâ€micrometerâ€sized uranium particles by laser ablation coupled with multiâ€collector inductively coupled plasma mass spectrometry. Rapid Communications in Mass Spectrometry, 2019, 33, 419-428.	1.5	9
26	Structural and thermodynamic study of Cs3Na(MoO4)2: Margin to the safe operation of sodium cooled fast reactors. Journal of Solid State Chemistry, 2019, 269, 1-8.	2.9	4
27	Dissolution kinetics of monazite LnPO4 (Ln = La to Gd): A multiparametric study. Applied Geochemistry, 2018, 93, 81-93.	3.0	25
28	Effect of powder morphology on sintering kinetics, microstructure and mechanical properties of monazite ceramics. Journal of the European Ceramic Society, 2018, 38, 227-234.	5.7	25
29	Synthesis of size-controlled UO2 microspheres from the hydrothermal conversion of U(iv) aspartate. CrystEngComm, 2018, 20, 7749-7760.	2.6	21
30	Thermodynamics and Stability of Rhabdophanes, Hydrated Rare Earth Phosphates REPO4 · n H2O. Frontiers in Chemistry, 2018, 6, 604.	3.6	27
31	Monazite, rhabdophane, xenotime & churchite: Vibrational spectroscopy of gadolinium phosphate polymorphs. Spectrochimica Acta - Part A: Molecular and Biomolecular Spectroscopy, 2018, 205, 85-94.	3.9	49
32	Solubility product of the thorium phosphate hydrogen-phosphate hydrate (Th 2 (PO 4 ) 2 (HPO 4 )·H 2) Tj ETQqO	9.8 rgBT	/9verlock 1
33	Thorium aspartate tetrahydrate precursor to ThO 2 : Comparison of hydrothermal and thermal conversions. Journal of Nuclear Materials, 2017, 487, 331-342.	2.7	19
34	In pursuit of the rhabdophane crystal structure: from the hydrated monoclinic LnPO 4 .0.667H 2 O to the hexagonal LnPO 4 (Ln = Nd, Sm, Gd, Eu and Dy). Journal of Solid State Chemistry, 2017, 249, 221-227.	2.9	42

35	Densification behavior and microstructure evolution of yttrium-doped ThO 2 ceramics. Journal of the European Ceramic Society, 2017, 37, 3381-3391.	5.7	14
36	Structural and thermodynamic study of dicesium molybdate Cs2Mo2O7: Implications for fast neutron reactors. Journal of Solid State Chemistry, 2017, 253, 89-102.	2.9	20

#	Article	IF	CITATIONS
37	Incorporation of thorium in the rhabdophane structure: Synthesis and characterization of Pr 1-2x Ca x Th x PO 4 ·nH 2 O solid solutions. Journal of Nuclear Materials, 2017, 492, 88-96.	2.7	14
38	Synthesis and Direct Sintering of Nanosized (M <sup>IV</sup> ,M <sup>III</sup> )O <sub>2â€∢i&gt;x</sub> Hydrated Oxides as Electrolyte Ceramics. ChemPhysChem, 2017, 18, 2666-2674.	2.1	3
39	Novel approaches for the <i>in situ</i> study of the sintering of nuclear oxide fuel materials and their surrogates. Radiochimica Acta, 2017, 105, 879-892.	1.2	9
40	High-temperature electron microscopy study of ThO 2 microspheres sintering. Journal of the European Ceramic Society, 2017, 37, 727-738.	5.7	25
41	In Situ Study of CeO2 Microspheres Sintering Using HT-ESEM. Microscopy and Microanalysis, 2016, 22, 62-63.	0.4	0
42	Determination of the Solubility of Rhabdophanes LnPO <sub>4</sub> ·0.667H <sub>2</sub> O (Ln = La to) Tj E	FQq0,00 r 2.0	gBT_/Overlock
43	Preparation, characterization and sintering of yttrium-doped ThO2 for oxygen sensors applications. Journal of Alloys and Compounds, 2016, 689, 374-382.	5.5	19
44	The effect of the synthesis route of monazite precursors on the microstructure of sintered pellets. Progress in Nuclear Energy, 2016, 92, 298-305.	2.9	17
45	Energetics of a Uranothorite (Th <sub>1–<i>x</i></sub> U <sub><i>x</i></sub> SiO <sub>4</sub> ) Solid Solution. Chemistry of Materials, 2016, 28, 7117-7124.	6.7	31
46	Incorporation of Thorium in the Zircon Structure Type through the Th <sub>1–<i>x</i></sub> Er <sub><i>x</i></sub> (SiO <sub>4</sub> ) <sub>1–<i>x</i></sub> (PO <sub>4Thorite–Xenotime Solid Solution. Inorganic Chemistry, 2016, 55, 11273-11282.</sub>	sub#)@sub	›> <i⊉&< i=""></i⊉&<>
47	Charged defects during alpha-irradiation of actinide oxides as revealed by Raman and luminescence spectroscopy. Nuclear Instruments & Methods in Physics Research B, 2016, 374, 67-70.	1.4	26
48	Vibrational spectroscopy of synthetic analogues of ankoleite, chernikovite and intermediate solid solution. Spectrochimica Acta - Part A: Molecular and Biomolecular Spectroscopy, 2016, 156, 143-150.	3.9	21
49	From in Situ HT-ESEM Observations to Simulation: How Does Polycrystallinity Affects the Sintering of CeO <sub>2</sub> Microspheres?. Journal of Physical Chemistry C, 2016, 120, 386-395.	3.1	27
50	First experimental determination of the solubility constant of coffinite. Geochimica Et Cosmochimica Acta, 2016, 181, 36-53.	3.9	35
51	Thermodynamics of formation of coffinite, USiO <sub>4</sub> . Proceedings of the National Academy of Sciences of the United States of America, 2015, 112, 6551-6555.	7.1	72
52	Catalytic dissolution of ceria–lanthanide mixed oxides provides environmentally friendly partitioning of lanthanides and platinum. Hydrometallurgy, 2015, 151, 107-115.	4.3	10
53	An original precipitation route toward the preparation and the sintering of highly reactive uranium cerium dioxide powders. Journal of Nuclear Materials, 2015, 462, 173-181.	2.7	25
54	Coffinite, USiO <sub>4</sub> , Is Abundant in Nature: So Why Is It So Difficult To Synthesize?. Inorganic Chemistry, 2015, 54, 6687-6696.	4.0	38

#	Article	IF	CITATIONS
55	From uranium(IV) oxalate to sintered UO 2 : Consequences of the powders' thermal history on the microstructure. Journal of the European Ceramic Society, 2015, 35, 4535-4546.	5.7	25
56	In situ HT-ESEM study of crystallites growth within CeO2 microspheres. Ceramics International, 2015, 41, 14703-14711.	4.8	18
57	Dissolution of Th1â^'U O2: Effects of chemical composition and microstructure. Journal of Nuclear Materials, 2015, 457, 304-316.	2.7	35
58	Effect of hydration and thermal treatment on ceria surface using non-intrusive techniques. Journal of Nuclear Materials, 2014, 444, 359-367.	2.7	8
59	High-temperature behavior of dicesium molybdate Cs2MoO4: Implications for fast neutron reactors. Journal of Solid State Chemistry, 2014, 215, 225-230.	2.9	22
60	Chemical and mineralogical modifications of simplified radioactive waste calcine during heat treatment. Journal of Nuclear Materials, 2014, 448, 8-19.	2.7	8
61	From thorite to coffinite: A spectroscopic study of Th1â°'xUxSiO4 solid solutions. Spectrochimica Acta - Part A: Molecular and Biomolecular Spectroscopy, 2014, 118, 302-307.	3.9	29
62	Dissolution of uranium mixed oxides: The role of oxygen vacancies vs the redox reactions. Progress in Nuclear Energy, 2014, 72, 101-106.	2.9	16
63	Environmental SEM monitoring of Ce <sub>1â^'x</sub> Ln <sub>x</sub> O <sub>2â^'x/2</sub> mixed-oxide microstructural evolution during dissolution. Journal of Materials Chemistry A, 2014, 2, 5193-5203.	10.3	52
64	Monoclinic Form of the Rhabdophane Compounds: REEPO <sub>4</sub> ·0.667H <sub>2</sub> O. Crystal Growth and Design, 2014, 14, 5090-5098.	3.0	61
65	Preparation and characterisation of uranium oxides with spherical shapes and hierarchical structures. CrystEngComm, 2014, 16, 6944-6954.	2.6	30
66	Dilatometric study of U1â^'xAmxO2±δ and U1â^'xCexO2±δ reactive sintering. Journal of Nuclear Materials, 2013, 441, 40-46.	2.7	18
67	Purification of uranothorite solid solutions from polyphase systems. Journal of Nuclear Materials, 2013, 441, 73-83.	2.7	17
68	Solubility properties of synthetic and natural meta-torbernite. Journal of Nuclear Materials, 2013, 442, 195-207.	2.7	23
69	From Uranothorites to Coffinite: A Solid Solution Route to the Thermodynamic Properties of USiO <sub>4</sub> . Inorganic Chemistry, 2013, 52, 6957-6968.	4.0	33
70	Versatile Monazite: Resolving geological records and solving challenges in materials science: Monazite as a promising long-term radioactive waste matrix: Benefits of high-structural flexibility and chemical durability. American Mineralogist, 2013, 98, 833-847.	1.9	151
71	Combining in situ HT-ESEM observations and dilatometry: An original and fast way to the sintering map of ThO2. Materials Chemistry and Physics, 2013, 137, 742-749.	4.0	32
72	The Flexible Ba <sub>7</sub> UM <sub>2</sub> S <sub>12.5</sub> O <sub>0.5</sub> (M = V, Fe) Compounds: Syntheses, Structures and Spectroscopic, Resistivity, and Electronic Properties. Inorganic Chemistry, 2013, 52, 12057-12063.	4.0	9

#	Article	IF	CITATIONS
73	Kinetics of Structural and Microstructural Changes at the Solid/Solution Interface during Dissolution of Cerium(IV)–Neodymium(III) Oxides. Journal of Physical Chemistry C, 2012, 116, 12027-12037.	3.1	16
74	<i>In Situ </i> <scp>HT</scp> â€ <scp>ESEM</scp> Observation of <scp><scp>CeO</scp></scp> <sub>2</sub> Grain Growth During Sintering. Journal of the American Ceramic Society, 2012, 95, 3683-3690.	3.8	24
75	Catalytic dissolution of ceria under mild conditions. Journal of Materials Chemistry, 2012, 22, 14734.	6.7	29
76	Triclinic–Cubic Phase Transition and Negative Expansion in the Actinide IV (Th, U, Np, Pu) Diphosphates. Inorganic Chemistry, 2012, 51, 4314-4322.	4.0	27
77	Synthesis and characterization of Th1â^'xLnxO2â^'x/2 mixed-oxides. Materials Research Bulletin, 2012, 47, 4017-4025.	5.2	51
78	Dissolution of Cerium(IV)–Lanthanide(III) Oxides: Comparative Effect of Chemical Composition, Temperature, and Acidity. Inorganic Chemistry, 2012, 51, 3868-3878.	4.0	44
79	Multiparametric study of Th1â^'xLnxO2â^'x/2 mixed oxides dissolution in nitric acid media. Journal of Nuclear Materials, 2012, 429, 237-244.	2.7	22
80	Preparation and characterization of synthetic Th0.5U0.5SiO4 uranothorite. Progress in Nuclear Energy, 2012, 57, 155-160.	2.9	27
81	Dynamic aspects of cerium dioxide sintering: HT-ESEM study of grain growth and pore elimination. Journal of the European Ceramic Society, 2012, 32, 353-362.	5.7	26
82	Calcined resin microsphere pelletization (CRMP): A novel process for sintered metallic oxide pellets. Journal of the European Ceramic Society, 2012, 32, 3199-3209.	5.7	37
83	Multiparametric Dissolution of Thorium–Cerium Dioxide Solid Solutions. Inorganic Chemistry, 2011, 50, 11702-11714.	4.0	65
84	Stability and Structural Evolution of Ce <sup>IV</sup> <sub>1–<i>x</i>/sub&gt;Ln<sup>III</sup><sub><i>x</i></sub>O<sub>2–<i>x</i>/2</sub> Solid Solutions: A Coupled μ-Raman/XRD Approach. Inorganic Chemistry, 2011, 50, 7150-7161.</sub>	4.0	109
85	Influence of Crystallization State and Microstructure on the Chemical Durability of Cerium–Neodymium Mixed Oxides. Inorganic Chemistry, 2011, 50, 9059-9072.	4.0	60
86	How To Explain the Difficulties in the Coffinite Synthesis from the Study of Uranothorite?. Inorganic Chemistry, 2011, 50, 11117-11126.	4.0	33
87	Negative thermal expansion in Th2O(PO4)2. Materials Research Bulletin, 2011, 46, 1777-1780.	5.2	14
88	Occurence of an Octanuclear Motif of Uranyl Isophthalate with Cation–Cation Interactions through Edge-Sharing Connection Mode. Inorganic Chemistry, 2011, 50, 6243-6249.	4.0	89
89	Tetrameric entity resulting from two distinct dinuclear uranyl-centered motifs bridged through μ2-OH and pyridazine-3,6-dicarboxylate. Inorganic Chemistry Communication, 2011, 14, 429-432.	3.9	24
90	Crystal chemistry of the monazite structure. Journal of the European Ceramic Society, 2011, 31, 941-976.	5.7	318

#	Article	IF	CITATIONS
91	Preparation of morphology controlled Th1â^'xUxO2 sintered pellets from low-temperature precursors. Powder Technology, 2011, 208, 454-460.	4.2	54
92	Kinetics of dissolution of thorium and uranium doped britholite ceramics. Journal of Nuclear Materials, 2010, 404, 33-43.	2.7	37
93	X-Ray Diffraction and μ-Raman Investigation of the Monoclinic-Orthorhombic Phase Transition in Th <sub>1â^²<i>xx</i></sub> U <sub><i>xx</i></sub> (C <sub>2</sub> O <sub>4</sub> ) <sub>2</sub> ·2H <sub>2</sub> 2 Solid Solutions. Inorganic Chemistry, 2010, 49, 1921-1931.	subøO	60
94	Preparation, sintering and leaching of optimized uranium thorium dioxides. Journal of Nuclear Materials, 2009, 385, 400-406.	2.7	55
95	Synthesis and characterization of coffinite. Journal of Nuclear Materials, 2009, 393, 449-458.	2.7	46
96	Synthesis, Raman and Rietveld analysis of thorium diphosphate. Journal of Solid State Chemistry, 2008, 181, 3352-3356.	2.9	25
97	Preparation of Optimized Uranium and Thorium Bearing Brabantite or Monazite/Brabantite Solid Solutions. Journal of the American Ceramic Society, 2008, 91, 3673-3682.	3.8	50
98	Comparative Behavior of Britholites and Monazite/Brabantite Solid Solutions during Leaching Tests: A Combined Experimental and DFT Approach. Inorganic Chemistry, 2008, 47, 10971-10979.	4.0	56
99	Hydrothermal Method of Preparation of Actinide(IV) Phosphate Hydrogenphosphate Hydrates and Study of Their Conversion into Actinide(IV) Phosphate Diphosphate Solid Solutions. Inorganic Chemistry, 2007, 46, 10390-10399.	4.0	15
100	Actinide solubility-controlling phases during the dissolution of phosphate ceramics. Journal of Nuclear Materials, 2007, 362, 451-458.	2.7	80
101	Crystal structures of Th(OH)PO4, U(OH)PO4 and Th2O(PO4)2. Condensation mechanism of MIV(OH)PO4 (M=Th, U) into M2O(PO4)2. Solid State Sciences, 2007, 9, 619-627.	3.2	41
102	Synthesis, Characterization, Sintering, and Leaching of β-TUPD/Monazite Radwaste Matrices. Inorganic Chemistry, 2006, 45, 220-229.	4.0	75
103	Behavior of thorium–uranium (IV) phosphate–diphosphate sintered samples during leaching tests. Part I – Kinetic study. Journal of Nuclear Materials, 2006, 349, 291-303.	2.7	52
104	Behavior of thorium–uranium (IV) phosphate–diphosphate sintered samples during leaching tests. Part II. Saturation processes. Journal of Nuclear Materials, 2006, 349, 304-316.	2.7	50
105	Improvement of the preparation of sintered pellets of thorium phosphate-diphosphate and associated solid solutions from crystallized precursors. Journal of Nuclear Materials, 2006, 352, 209-216.	2.7	22
106	From thorium phosphate hydrogenphosphate hydrate to β-thorium phosphate diphosphate: Structural evolution to a radwaste storage ceramic. Journal of Solid State Chemistry, 2006, 179, 3007-3016.	2.9	17
107	Investigation in thorium phosphate by NMR II-phosphorus dipolar networks. Solid State Nuclear Magnetic Resonance, 2006, 29, 294-304.	2.3	5
108	Investigation in hydrated thorium phosphates by NMR I-relation proton phosphorus. Solid State Nuclear Magnetic Resonance, 2006, 30, 29-44.	2.3	0

#	Article	IF	CITATIONS
109	Kinetic and Thermodynamic Study of the Chemistry of Neoformed Phases during the Dissolution of Phosphate Based Ceramics. Materials Research Society Symposia Proceedings, 2006, 985, 1.	0.1	0
110	Separation of uranium(VI) from tri- and tetravalent elements in phosphoric acid solutions. Radiochimica Acta, 2006, 94, .	1.2	0
111	Hydrothermal Methods as a New Way of Actinide Phosphate Preparation. Materials Research Society Symposia Proceedings, 2006, 985, 1.	0.1	2
112	Characterization of the thorium phosphate-hydrogenphosphate hydrate (TPHPH) and study of its transformation into the thorium phosphate-diphosphate (I²-TPD). Materials Research Bulletin, 2005, 40, 2225-2242.	5.2	43
113	Synthesis and characterization of uranium (IV) phosphate-hydrogenphosphate hydrate and cerium (IV) phosphate-hydrogenphosphate hydrate. Journal of Solid State Chemistry, 2005, 178, 1054-1063.	2.9	39
114	Synthesis and characterization of low-temperature precursors of thorium–uranium (IV) phosphate–diphosphate solid solutions. Journal of Nuclear Materials, 2004, 335, 397-409.	2.7	21
115	Immobilisation of actinides in phosphate matrices. Comptes Rendus Chimie, 2004, 7, 1141-1152.	0.5	107
116	Sintering of β-Thoriumâ^'Uranium(IV) Phosphateâ^'Diphosphate Solid Solutions from Low-Temperature Precursors. Chemistry of Materials, 2004, 16, 3357-3366.	6.7	31
117	Preparation and characterization of lanthanum–gadolinium monazites as ceramics for radioactive waste storage. New Journal of Chemistry, 2003, 27, 957-967.	2.8	142
118	Study of Actinides Incorporation in Thorium Phosphate-Diphosphate/Monazite Based Ceramics. Materials Research Society Symposia Proceedings, 2003, 802, 111.	0.1	2